Brain Connectivity

DOI: 10.1089/brain.2016.0483

Integration and Segregation of Default Mode Network Resting-state Functional Connectivity in Transition-age Males with High-functioning Autism Spectrum Disorder: A Proof of Concept Study

Gagan Joshi, MD[1,2,3], Sheeba Arnold Anteraper, PhD[1,3], Kaustubh R. Patil, PhD[1], Meha Semwal, BS[1], Rachel L. Goldin, BA[1], Stephannie L. Furtak, BA[1], Xiaoqian Jenny Chai, PhD[4], Zeynep M. Saygin, PhD[3], John D. E. Gabrieli, PhD[3,5], Joseph Biederman, MD[1,2], and Susan Whitfield-Gabrieli[3,5]

[1]Alan and Lorraine Bressler Clinical and Research Program for Autism Spectrum Disorder, Massachusetts General Hospital, Boston MA; [2]Department of Psychiatry, Harvard Medical School, Boston MA; [3]McGovern Institute for Brain Research, Massachusetts Institute of Technology, Cambridge MA; [4]Departments of Neurology, Johns Hopkins University, Baltimore, MD; [5]Department of Brain and Cognitive Sciences, Massachusetts Institute of Technology, Cambridge, MA.

Corresponding Author:

Gagan Joshi, MD

Alan and Lorraine Bressler Clinical and Research Program for Autism Spectrum Disorder, Massachusetts General Hospital, Boston MA

Department of Psychiatry, Harvard Medical School, Boston MA

McGovern Institute for Brain Research, Massachusetts Institute of Technology, Cambridge MA Email: Joshi.Gagan@mgh.harvard.edu

Running Head: Resting State Functional Connectivity in ASD

ABSTRACT

Objectives: To assess the resting-state functional connectivity (RsFc) profile of the default mode network (DMN) in transition-age males with autism spectrum disorder (ASD).

Methods: Resting-state blood oxygen level dependent functional MRI (fMRI) data were acquired from adolescent and young adult males with high-functioning ASD (N=15) and from age-, sex-, and IQ-matched healthy controls (HC; N=16).

The DMN was examined by assessing the positive and negative RsFc correlations of an average of the literature-based conceptualized major DMN nodes (medial prefrontal cortex [mPFC], posterior cingulate cortex, bilateral angular and inferior temporal gyrii regions). RsFc data analysis was performed using a seed driven approach.

Results: ASD was characterized by an altered pattern of RsFc in the DMN. The ASD group exhibited a weaker pattern of intra- and extra- DMN positive and negative RsFc correlations respectively. In ASD the strength of intra-DMN coupling was significantly reduced with the mPFC and the bilateral angular gyrii regions. In addition, the polarity of the extra-DMN correlation with the right hemispheric task-positive regions of fusiform gyrus and supramarginal gyrus was reversed from typically negative to positive in the ASD group. A wide variability was observed in the presentation of the RsFc profile of the DMN in both HC and ASD groups that revealed a distinct pattern of sub-grouping using pattern recognition analyses.

Conclusions: These findings imply that the functional architecture profile of the DMN is altered in ASD with weaker than expected integration and segregation of the DMN RsFc. Future studies with larger sample sizes are warranted.

Key Words: autism spectrum disorder, resting-state fMRI, default mode network

Brain Connectivity
Integration and Segregation of Default Mode Network Resting-state Functional Connectivity in Transition-age Males with High-functioning Autism Spectrum Disorder: A Proof of Concept Study (DOI: 10.1089/brain.2016.0483)
This paper has been peer-reviewed and accepted for publication, but has yet to undergo copyediting and proof correction. The final published version may differ from this proof.

INTRODUCTION

Autism spectrum disorder (ASD) is a highly morbid neurodevelopmental disorder characterized by varying degrees of deficits in social-emotional functioning along with restricted, repetitive behaviors (APA, 2013) that is estimated to affect up to 2% of children and adolescents in the general population (Blumberg et al., 2013). ASD in intellectually capable individuals is characterized by impaired social and emotional awareness, motivation, and reciprocity, cognitive rigidity, and limited perspective taking and introspective ability (Ben Shalom et al., 2006; Blakemore & Choudhury, 2006; Ebisch et al., 2011; Hill et al., 2004; Rieffe et al., 2007; Salmi et al., 2013). The clinical presentation of ASD is highly heterogeneous and the diagnosis of ASD is often delayed, more so in intellectually-capable populations where social impairments may not fully manifest until developmentally expected social demands exceed limited capacities (APA, 2013).

While there is strong evidence that autism is associated with abnormal brain development, the nature of the aberrant neural functioning is not well characterized (Muller et al., 2011; Nicolson & Szatmari, 2003). Considering the central role that social deficits play in ASD, neuroimaging research focused on the brain regions associated with social processing is of particular interest. Improved understanding of the neural correlates may help elucidate neural mechanisms and help identify biomarkers that could aid earlier diagnosis of ASD, prior to the emergence of clinical markers, and possibly inform pharmaco-therapeutic interventions.

Based on the extant literature (Adolphs, 2009; Blakemore, 2008; Di Martino et al., 2009; Frith & Frith, 2007; Mitchell, 2009; Olson et al., 2007), the major brain regions that are typically identified as components of a social processing network include the prefrontal cortical (PFC) regions (medial PFC [mPFC] and orbitofrontal cortex), the limbic regions [regions of medial temporal lobe (amygdalae and anterior hippocampi) and cingulate cortex (anterior & posterior cingulate cortex {ACC & PCC})], anterior temporal lobes, temporo-parietal regions (lateral fusiform gyrii [FG], temporo-parietal junction [TPJ]), and anterior insulae (AI). Emerging neuroimaging literature on functional connectivity (Fc) in autism has identified social-task-related hypoactivation of brain regions that sub-serve the social-emotional brain networks including the mPFC, ACC, PCC, angular gyrus (AG), right (Rt.) AI, and left (Lt.) FG (Di Martino et al., 2009).

Brain Connectivity
Integration and Segregation of Default Mode Network Resting-state Functional Connectivity in Transition-age Males with High-functioning Autism Spectrum Disorder: A Proof of Concept Study (DOI: 10.1089/brain.2016.0483)
This paper has been peer-reviewed and accepted for publication, but has yet to undergo copyediting and proof correction. The final published version may differ from this proof.

Resting-state (Rs) fMRI assesses intrinsic functional brain activity in the absence of an overt task (task-independent) (Biswal et al., 1995; Fox et al., 2005; Greicius et al., 2003; Lowe et al., 2000). Brain regions that are simultaneously active during Rs exhibit a positive temporal correlation of associated blood oxygen level dependent (BOLD) signals, together constituting intrinsic functional networks. Functional networks identified by Rs-fMRI have been shown to be robust and reliable and can thus provide useful information about brain organization differences across different clinical populations and during development (Dosenbach et al., 2010; Seeley et al., 2009). A key advantage of Rs analysis over task-based measures is the absence of possible confounds associated with underlying differences in task performance or in the way the task is executed.

The default mode network (DMN) is the one of the most extensively studied resting-state functional connectivity (RsFc) networks. The DMN is an integrated system that supports self-monitoring and social, emotional, interpersonal, and introspective processes (Raichle et al., 2001). It is an endogenously mediated network that is activated at rest and during social/emotional tasks while deactivated by cognitively demanding non-social tasks. The DMN is involved in many of the processes that are compromised in individuals with autism, including social and interpersonal cognition (Buckner et al., 2008; Uddin, 2011).

Intrinsic functional brain connectivity is altered in autism with evidence of both hypo- and hyper-connectivity, findings that are possibly reflective of the complex phenotype of the disorder. Although the literature on RsFc of the DMN in ASD suggests both hypo- and hyper-connectivity within the network and reduced inter-network connectivity (Assaf, et al., 2010; Barttfeld et al., 2012; Di Martino et al., 2013; Doyle-Thomas et al., 2015; Eilam-Stock et al., 2014; Kennedy & Courchesne, 2008; Lynch et al., 2013; Monk et al., 2009; Mueller et al., 2013; Starck et al., 2013; Uddin et al., 2013; von dem Hagen et al., 2013; Washington et al., 2014; Weng et al., 2010; Wiggins et al., 2011; Ypma et al., 2016; Zhao et al., 2016), the most consistent finding is of reduced RsFc within the DMN with weaker coherence of RsFc between the posterior and anterior subsystems (Assaf et al., 2010; Di Martino et al., 2013; Doyle-Thomas et al., 2015; Eilam-Stock et al., 2014; Kennedy & Courchesne, 2008; Monk et al., 2009; Starck et al., 2013; von dem Hagen et al., 2013; Washington et al., 2014; Weng et al., 2010; Wiggins et al., 2011; Ypma et al., 2016; Zhao et al., 2016).

The inter-network RsFc is derived from varying levels of negative correlations, also known as anti-correlations. While positive correlations serve an integrative role in combining neuronal activity sub-serving similar function, anti-correlations serve a differentiating role segregating neuronal processes sub-serving competing functions, a phenomenon typically shared between the task-negative (TN) network i.e., the DMN and brain networks activated during non-social task performance (task-positive [TP] networks). Typically, the strength of the DMN integration (positive correlation) and segregation (anti-correlation) with the TP network correlates with the level of social-emotional maturity and enhances during early adolescence stage of development (Doyle-Thomas et al., 2015; Sherman et al., 2014; Washington et al., 2014).

RsFc studies in autism have generally focused on examining the positive correlation profile from various seed regions. While study of positive correlations of functional neural activity sheds light on the integrative role of neural functions, it fails to offer information on the concurrent anti-correlated functional brain activity, which offers understanding of the functional segregation between RsFc networks. Between-network connectivity may offer insight into the extent with which these networks interact and share functionally relevant information. For instance, social deficits in autism may be due to a lack of anti-correlation between TN (DMN) and TP networks, leading to failure of suppression and related interference of TP networks during social processing, ultimately resulting in social impairments. However, given anti-correlations have not been studied in conjunction with positive functional correlations in ASD, this hypothesis remains largely unexplored.

To date, only two RsFc studies in autism have examined anti-correlations in ASD. Kennedy & Courchesne (2008) examined anti-correlations in the context of applying global signal regression (GSR), which introduces artefactual anti-correlations to the results (Kennedy & Courchesne, 2008; Anderson et al., 2011a; Murphy et al., 2009). Anderson and colleagues (2011a) examined Rs anti-correlations without applying GSR in a wide age range sample of youth and adults with ASD; however, as the seed regions spanned through the entire gray matter, the weaker anti-correlations reported within the ASD group were not specific to the DMN (Anderson et al., 2011b; Murphy et al., 2009). Thus, to the best of our knowledge, no previous study has concurrently examined both positive and negative correlations of intrinsic Fc of the DMN in ASD.

To this end, we characterized the RsFc profile of the DMN in a selected sample of transition age male individuals with ASD by simultaneously examining RsFc for both the positive as well as the negative correlations. We conducted a seed-driven whole brain correlation analysis of regions of interest (ROIs) anchored around averages of the literature-based conceptualized major DMN nodes including mPFC, PCC, and bilateral (Bl.) AG, and inferior temporal gyrii (Raichle, 2011). Based on the extant literature, we hypothesized that the profile of the DMN in ASD would reveal a functional dysconnectivity pattern that replicates previous findings of reduced functional integration and, in addition, would document reduced functional segregation of the DMN in particular with the TP regions (i.e., how the two networks are distinct from each other). Furthermore, we explored the applicability of pattern recognition approaches for acquiring additional insights into the RsFc characteristics and their relationship to the ASD. We used unsupervised machine learning and graph theoretical analyses to study the diversity of the connectivity patterns and identify subtypes of atypical connectivity between the ROIs that may potentially serve as diagnostic neural markers. As an exploratory hypothesis, we examined the between-subjects diversity in DMN connectivity that is well documented in populations with ASD.

MATERIALS AND METHODS

Ascertainment of Study Participants

ASD participants were recruited from referrals to a specialized ambulatory program for autism spectrum disorder and to a child & adolescent psychiatry ambulatory care clinic at the MGH. The age-, sex-, and IQ (Intelligence Quotient) -matched healthy controls (HC) were recruited by advertising for the study. Excluded were participants with psychosis, autism, inadequate command of the English language, a Full Scale IQ < 80, or major sen-sorimotor disabilities (paralysis, deafness, blindness). All participants completed the assessment as detailed below after providing written informed consent following complete description of the study. Human research committees at Massachusetts General Hospital and the Massachusetts Institute of Technology approved this study. To further investigate

Brain Connectivity
Integration and Segregation of Default Mode Network Resting-state Functional Connectivity in Transition-age Males with High-functioning Autism Spectrum Disorder: A Proof of Concept Study (DOI: 10.1089/brain.2016.0483)
This paper has been peer-reviewed and accepted for publication, but has yet to undergo copyediting and proof correction. The final published version may differ from this proof.

the reproducibility of our findings we applied identical analysis on the open-access ABIDE dataset (Autism Brain Imaging Data Exchange; N=59) contributed by principal investigator Michal Assaf, M.D (Olin Neuropsychiatry Research Center [ONRC], Institute of Living, Hartford Hospital & Yale School of Medicine, Dept. of Psychiatry). Detailed information on the assessment and neuroimaging procedures is provided in the release/website (http://fcon_1000.projects.nitrc.org/indi/abide/).

Assessment Procedures

Full-scale IQ of all study participants (ASD and HC) was assessed with the Vocabulary and Matrix Reasoning subtests of the Wechsler Abbreviated Scale of Intelligence Scale (Wechsler, 1999). The observer-rated Edinburgh Handedness Inventory was administered to assess the Rt. or Lt. laterality of dominance in all the study participants (Oldfield, 1971). Socioeconomic status was measured using the four-factor Hollingshead index (Hollingshead, 1975).

ASD Participants: All ASD participants received a neuropsychological assessment, a structured diagnostic interview, and a clinical psychiatric diagnostic interview. The diagnosis of ASD was established by a comprehensive psychiatric evaluation conducted by a board-certified psychiatrist experienced in evaluating ASD (GJ). The psychiatric diagnostic interview was conducted with the subject and, if available, their parent/guardian(s) and incorporated information from multiple sources when available (e.g., psychiatric records, social services). Based on this clinical evaluation, all ASD subjects met Diagnostic and Statistical Manual of Mental Disorders - Fourth Edition (DSM-IV) diagnostic criteria for autistic disorder, Asperger's disorder, or PDD-NOS.

Youth (<18 years old) with ASD were evaluated by administering the Kiddie Schedule for Affective Disorders and Schizophrenia-Epidemiological Version (K-SADS-E) (Orvaschel, 1994; Orvaschel & Puig-Antich, 1987) to the care-taker (parent/guardian), usually the mother. The K-SADS-E is a semi-structured interview that generates current and lifetime Axis-I diagnoses according to DSM-III-R/IV criteria (APA, 1987, 1994) in children and adolescents. It has been shown to possess acceptable test–retest and inter-rater reliabilities (Chambers et al., 1985). All adults (≥18 years old) with ASD were evaluated by administering the Structured Clinical Interview for DSM-IV (SCID), supplemented with modules from the K-SADS-E to assess childhood diagnoses (First et al., 1996). The SCID was

administered to the patients themselves as well as a parent/guardian when available. We combined data from both the direct and indirect structured diagnostic interviews by considering a diagnostic criterion positive if it was endorsed in either interview.

Healthy Controls: HC were screened for ASD traits with the Social Communication Questionnaire (Berument et al., 1999; Rutter et al., 2003).

Neuroimaging Procedures

Data Acquisition: Neuroimaging data were acquired on a Siemens 3T scanner, MAGNETOM Trio, a Tim System (Siemens AG, Healthcare Sector, Erlangen, Germany), using a commercially available receive-only 32 Channel radio frequency brain array head coil (Siemens AG, Healthcare Sector, Erlangen, Germany). Participants underwent a resting functional MRI scan for six minutes with the instructions, "Keep your eyes open and think of nothing in particular." Resting scan images were obtained parallel to AC-PC, covering the entire brain (interleaved EPI sequence, T2*- weighted images; repetition time = 6 sec, echo time = 30 ms, flip angle = 90°, 67 slices with 2x2x2 mm^3 voxels). T1-weighted whole brain structural images were acquired using MPRAGE sequence (TR/TE/TI/Flip Angle were 2530 ms/3.39 ms/1100 ms/7°, 256 x 256 x 176 voxels, 1 x 1.3-mm in-plane resolution, 1.3-mm slice thickness). Online prospective acquisition correction (PACE) was applied to the EPI sequence to mitigate artifacts due to head motion (Thesen et al., 2000). Gradient adjusted PACE data set was used for further analysis.

ABIDE Dataset: Resting scan images were obtained on 3T Siemens Skyra (repetition time = 0.475 sec, echo time = 30 ms, flip angle = 60°, 3x3x3 mm^3 voxels, Multiband factor of 8). T1-weighted whole brain structural images were acquired using MPRAGE sequence (TR/TE/TI/Flip Angle were 2200 ms/2.88 ms/794 ms/13°, 0.8x0.8x0.8 mm^3 voxels).

(Table-I)

Creation of Seeds of Interest: *A priori* seeds of interest for the DMN were independent of our data and were defined as spheres with 5-mm radius centered on previously published foci (Fox et al., 2005; Raichle, 2011) generated using WFU_PickAtlas (Maldjian et al., 2003). Seeds at the network level were comprised of the average of multiple seeds corresponding to the pre-defined seed-regions (listed in Table-I). The lateral parietal seed was located in the posterior subdivision of the AG (pAG) bilaterally, which is known to be more strongly

functionally correlated with the DMN nodes than the corresponding anterior subdivision (Caspers et al. 2006; Uddin et al., 2010).

Data Analysis: *Data Preprocessing*: Rs fMRI data were first preprocessed in SPM8 (Wellcome Department of Imaging Neuroscience, London, UK; http://www.fil.ion.ucl.ac.uk/spm), using standard spatial preprocessing steps. Data were slice-time and motion corrected, realigned, co-registered to structural scans, normalized to an MNI template, and spatially smoothed with 6-mm FWHM Gaussian kernel. *Motion artifact detection*: ART (http://www.nitrc.org/projects/artifact_detect) was used to identify outlier data points (TRs) defined as volumes that exceeded 3 z-normalized standard deviations away from mean global brain activation across the entire volume, or a composite movement threshold of 1 mm scan-to-scan frame wise displacement. There was no significant difference in the total number of outliers between groups. Mean number of outliers in the HC group was 4 and that in the ASD group was 7. In addition, there was no significant difference in the mean head motion parameters between groups (ASD=0.11 ±0.05 vs. HC=0.098±0.05; p=0.58). For the ABIDE dataset, a bit more conservative threshold of 0.5 for composite motion was used (scan-to-scan). Although there was no significant difference in the total number of valid scans per group, the maximum head movement in the ASD group was significantly more (p=0.05) compared to the ASD group. We have therefore regressed out the effect of maximum motion in the second-level analyses.

Connectivity Analysis: RsFc analysis was performed using a seed driven approach with in-house, custom software developed in Matlab,"Conn toolbox" (Whitfield-Gabrieli & Nieto-Castanon, 2012); http://www.nitrc.org/projects/conn/).

Each participant's structural image was segmented into white matter (WM), gray matter (GM), and cerebral spinal fluid (CSF) using SPM8 (Ashburner & Friston, 2005). To minimize partial volume effects with adjacent GM, the WM and CSF masks were eroded by one voxel and used as noise ROI. Instead of using global signal regression, the first 3 principal components of the signals from the eroded WM and CSF noise ROIs were removed with regression (Chai et al., 2012) through an anatomical Component based noise Correction approach (aCompCor; Behzadi et al., 2007). Finally, to minimize the effects of head motion

related confounds, we used the realignment parameters and their first order derivatives along with the motion outliers as regressors during denoising. A temporal band-pass filter of 0.009 Hz to 0.08 Hz was applied to the time series.

Statistical Analysis

Seed-voxel Whole Brain Correlation Analyses: First-level correlation maps were produced by extracting the residual BOLD time course from the average time-course of the *a priori* seed regions of interest, followed by computing Pearson's correlation coefficients between that time course and the time course of all other voxels. Correlation coefficients were then converted to normally distributed z-scores using the Fisher's transformation to allow for second-level General Linear Model analyses. Second-level between-group t-tests were performed for the correlations maps from the ASD and HC groups. An average of the six pre-defined DMN seeds served as the source region of interest. Both positive and negative correlations with the source were investigated. All reported clusters that survived a threshold of $p<0.005$ (height-level) and $p<0.05$ (corrected for Family Wise Error at the cluster-level) were used as regions of interest for further analysis. For the ABIDE dataset, group level ICA (Calhoun et al., 2001) was carried out in CONN to explore the DMN independent of seeds in order to take advantage of the superior temporal sampling (TR = 0.475s, 947 time points) of this dataset.

Pattern Recognition Analyses: *Machine learning analysis*: We used Gaussian mixture modeling (GMM) followed by the Bayesian information criterion for model selection (Fraley & Raftery, 2012) to perform unsupervised clustering analysis. We used the mclust package version 5.0.2 in the R statistical environment 3.2.0 (R Core Team, 2015). GMM fits a given number of Gaussian mixture components to the data. More components increase the number of free parameters, which often leads to a better fit at the expense of model complexity. The tradeoff between the model fit and complexity was controlled using the Bayesian information criterion (BIC) by penalizing models that are more complex (Fraley & Raftery, 2012). Note that mclust allows to fit models that impose a variety of constraints on the components, such as the orientation and shape of the Gaussians. We tested all the 14 models provided in the mclust package. We chose the final model that showed minimum BIC. The Fisher's Z transformed correlations between the mean of the DMN and

the regions that survived the second-level Fc analysis were used to describe each subject. In the final matrix with each subject representing a row, the feature vectors were normalized to have mean of zero and standard deviation of one, so that each ROI got equal importance. For visualization purposes, we performed principal components analysis (PCA) (Jolliffe, 2002) and retained the first two components. We used a nine-dimensional space - one dimension per ROI that showed significant difference (for exploratory purposes; height-threshold of $p<0.01$, cluster corrected at $p<0.05$ FDR-corrected) between ASD and controls - to represent each subject. In order to visualize the clustering results, i.e. whether the ASD and controls get separated, we performed PCA on this nine-dimensional data and plotted it using the first two dimensions. The standard "prcomp" function in the R statistical package was used to perform the PCA.

Graph Theoretical Analysis: For each subject we calculated the pairwise relationship between the ROIs as the Pearson correlation matrix between the corresponding averaged time series. First, we investigated the average connection strength. The upper triangle of the correlation matrix was Fisher's Z transformed and the absolute values were averaged. This gives a proxy measure for the total inter-ROI connectivity. To gain more insights into the inter-ROI connectivity patterns we utilized minimum spanning tree (MST) (Tewarie et al., 2015). MST provides a unique and mathematically efficient representation and has been previously utilized with MRI data (Stam, 2014). MST as acyclic graphs provides a concise representation of the relationship between the variables. The data is first represented as a fully connected graph for each subject with one node per ROI, and the edges between the nodes weighted with the Pearson correlation distance (one minus correlation). A MST algorithm then prunes some of the edges such that the graph remains connected while the sum of the distances of the remaining edges is minimized. This provides an interpretable graph topology with, in some sense, only the important connections retained. Finally, the specificity and sensitivity values were reported for the MST based discrimination between ASD and controls. Specificity was calculated as the proportion of controls (true negatives) that were correctly identified based on MST and sensitivity as the proportion of ASD (true positives) that were correctly identified out of the total ASD participants.

RESULTS

Clinical Characterization

(Table-II)

Participant Characterization: All ASD participants (N=15) in this study were native English-speaking, right-handed (with the exception of one participant), Caucasian males (age: mean=21.6 ±3.7; range=16-28 years) with intact intellectual capacity (IQ: mean=111 ±10; range=96-130). HC participants were significantly less frequently Caucasian (50% vs. 93%; p=0.02) and had a significantly higher mean IQ (123 ±9.2 vs. 111 ±10; p=0.001) than the ASD participants. For the ABIDE dataset, there were 24 ASD participants (20 males, mean age = 21.1 ±2.9; range = 18-31 years and 4 females, mean age = 24.4 ±1) and 35 HC (20 males, mean age = 24.2 ±3.5; range = 19-30 years and 15 females, mean age = 23.9 ±2.7). There was no significant difference (p=0.46) in IQ between the two groups (ASD: 114 ±12.4 (80-146) and HC: 111.2 ± 10(85-146)).

(Table-III)

Phenotypic Correlates: Among the ASD participants, 67% (10/15) were diagnosed with autistic disorder, 20% (3/15) Asperger's disorder, and 13% (2/15) PDD-NOS. On the structured diagnostic interview for psychopathology completed at enrollment, seven ASD participants were experiencing Attention-deficit/hyperactivity disorder (ADHD) and six were suffering from Major Depressive Disorder (MDD) (Table-III). The psychotropic treatment status of the 15 ASD participants at the time of scan was as following: 1) five ASD participants were medication naïve; five ASD participants were on monotherapy (selective serotonin reuptake inhibitors [SSRIs]=4; stimulant=1); the remaining five participants were on a combination of more than two psychotropic medications. SSRIs (8/10) and stimulants (5/10) were the most common class of psychotropic medications being taken by the ASD participants in this study.

Neural Characterization

(Figure-I.A & I.B)

Within-group ASD and HC Fc Maps: At the network level the Fc maps for the default mode - as derived from the average seed from the six *a priori* DMN nodes - in the HC were largely similar to what is typically expected. The intrinsic Fc architecture of the DMN in the

ASD group was atypical, in particular for: 1) the absence of positive correlation with the Lt. cerebellar lobule VIIa region and negative correlations with the Rt. hemispheric TP regions belonging to the lateral FG and associative visual cortex (aVC) and the posterior superior temporal gyrus (pSTG), the supramarginal gyrus (SMG) and primary auditory cortex (pAC); and 2) for the presence of positive correlation with the aforementioned TP regions and with the medial aspect of FG and secondary visual cortical (sVC) region in the Rt. hemisphere (Figure-I.A). Similar atypical Fc architecture of the DMN in ASD was also evident in the ABIDE dataset (Figure-I.B).

(Figure-II.A & II.B)

(Table-IV)

Between-group ASD and HC Fc Network Interactions: In the ASD group, relative to the HC group, the RsFc of the DMN seed exhibited: 1) significantly lower positive correlations with the Bl. AG regions, mPFC regions of anterior PFC (aPFC) and 2) significantly higher positive correlation with the Rt. hemispheric regions that include the lateral aVC/FG and the pSTG/SMG/pAC (Figure-II.A). Results are summarized in Table-IV.

For the ABIDE data set, distinctly lower or lack of anticorrelations in Rt. SMG and Rt. pSTG was apparent in the between-group comparison within the ASD group (Figure-II.B). In addition, the correlations analysis between the clinical severity of autism on total ADOS and RsFc of the whole brain (DMN component from group-ICA) revealed a significant positive correlations with DMN functional connectivity with the right hemisphere regions of SMG and pSTG (Figure III).

(*Figure-III*)

For exploratory analysis of the between-group differences that emerged from our dataset using pattern recognition analyses, a height-level threshold of $p<0.01$ ($p<0.05$ corrected for False Discovery Rate (FDR) at the cluster-level) was applied to the second-level between-group DMN seed-voxel whole brain correlation analyses. This allowed us to further investigate the source of the differences in RsFc. There were 9 regions that survived the significance test. The three regions that are typically anti-correlated with the DMN in HC were observed to join the DMN for the ASD group. Box plot representation of ASD versus controls on these nine regions that survived two-sample t-test is shown in Figure-IV. Additional ROIs that were identified, in addition to the ROIs identified at the

Brain Connectivity
Integration and Segregation of Default Mode Network Resting-state Functional Connectivity in Transition-age Males with High-functioning Autism Spectrum Disorder: A Proof of Concept Study (DOI: 10.1089/brain.2016.0483)
This paper has been peer-reviewed and accepted for publication, but has yet to undergo copyediting and proof correction. The final published version may differ from this proof.

higher threshold of significance, included mPFC regions of aPFC, perigenual ACC (pgACC) and Lt. cerebellar lobule VIIa (Crus I/II) with significantly lower positive correlations, and medial FG/sVC with significantly higher positive correlation.

(Figure-IV)

Pattern Recognition Analyses: As depicted in the box plot representation in Figure-IV there was marked variability in the individual results of the nine regions that survived the between-group second-level significance tests. These nine ROIs were subjected to clustering analysis.

Clustering Analysis: We clustered the pooled 15 ASD subjects and 16 HC subjects using the unsupervised machine learning method as described in the methods section. Using the Bayesian information criterion for model selection, we identified five clusters (Figure-V.A). Four of the clusters, two each in the ASD and HC group, were pure (they contained only ASD or HC subjects), whereas the remaining sub-cluster had both ASD and HC subjects.

Relationship between ROIs (MST Analysis): We probed whether the relationship between the ROIs differs between ASD and HC. We found that in the HC subjects the ROIs were significantly more tightly connected than in the ASD subjects (m=0.37 vs. m=0.26; t-test t(3.35, 19.06), p-value = 0.0033). To gain further insights into the inter-ROI connectivity, we investigated their connection topology using MST (see methods). We defined two types of ROIs based on their connectivity with the DMN; six positively correlated regions (TN network) and three negatively correlated regions (TP network). Based on the connectivity of those two types of regions within the MST for each subject, an atypical pattern of the TP network regions connecting with the TN network (DMN) regions was observed at a higher rate in the subjects with ASD than HC (10/15 [67%] vs. 1/16 [6%]; Figure-V.B).

(Figure-V.A & V.B)

DISCUSSION

This study addressed RsFc of the DMN in intellectually capable transition-age males with ASD. Findings in this study suggest that the architecture and strength of the DMN Fc is altered in ASD. The DMN in ASD was poorly integrated with reduced intra-DMN RsFc with

the mPFC and Bl. AG regions. In addition, there was significant failure of the DMN to functionally segregate from TP regions in the Rt. hemisphere, which were instead functionally integrated with the DMN, including the regions of FG, VC, AC, SMG, and pSTG. Thus the Fc architecture of the DMN in ASD was significantly altered with inclusion of the Rt. hemispheric TP regions of FG, VC, SMG, and AC. Notably, there was a broad inter-subject variability in the strength of the DMN RsFc with the brain regions that survived between-group differences. Moreover, based on the varying strengths of the DMN RsFc with brain regions of interest, the clustering analysis suggests presence of sub-groups with distinct neural profiles, consistent with the typically observed heterogeneous phenotypic expression of ASD. Our findings of weaker functional segregation of the DMN with the TP regions of SMG and pSTG in the Rt. hemisphere, were replicated by identical analysis in independent (ABIDE) data set. To ensure that there is an agreement between the two cohorts, we exported the cluster (Rt. SMG/pSTG) that survived the between-group comparison from ABIDE sample and used that as a mask for small volume correction in our dataset for ASD>HC comparison. There was a significant overlap of 24 clusters at a cluster-level significance of $p<0.05$ FWE corrected.

Within group functional architecture of DMN

The correlation maps for typically developing participants in this study were largely consistent with previous studies in healthy individuals. The functional architecture of DMN in the ASD individuals was atypical for lack of positive RsFc with the Lt. cerebellar region and aberrant positive RsFc with regions in the Rt. hemisphere that are typically anti-correlated with DMN, namely the FG, VC, AC, SMG, and pSTG. Atypical patterns of correlations and significant lack of anticorrelations were evident with the ABIDE dataset.

Integration of DMN in ASD (Positive-correlations)

Our finding of reduced intra-DMN RsFc in ASD is in line with the most consistently reported findings of intra-DMN hypo-connectivity in ASD (Assaf et al., 2010; Barttfeld et al., 2012; Di Martino et al., 2013; Doyle-Thomas et al., 2015; Eilam-Stock et al., 2014; Fishman et al., 2014; Kennedy & Courchesne, 2008; Lai et al., 2010; Monk et al., 2009; Rudie et al., 2012; Starck et al., 2013; von dem Hagen et al., 2013; Washington et al., 2014; Weng et al., 2010; Wiggins et al., 2011; Ypma et al., 2016; Zhao et al., 2016). Considering the substantial evidence supporting the view that the DMN mediates consideration of

Brain Connectivity
Integration and Segregation of Default Mode Network Resting-state Functional Connectivity in Transition-age Males with High-functioning Autism Spectrum Disorder: A Proof of Concept Study (doi: 10.1089/brain.2016.0483)

one's own thoughts and feelings, or self-referential processing (Johnson et al. 2002; Kelley et al. 2002; d'Argembeau et al. 2005; Moran et al. 2006; Northoff & Bermpohl 2004; Northoff et al. 2006; Whitfield-Gabrieli et al. 2011), the poor functional integration of the DMN may account for diminished capacity for self-referential processing in autism. As the DMN also facilitates a "state of readiness" to respond to environmental changes, reduced functional integration of DMN may also account for poor awareness and response to surroundings in ASD (Raichle & Gusnard, 2005).

Among the major nodes of DMN, the mPFC and Bl. AG were poorly integrated with the network in ASD. In particular, the aPFC region of mPFC were under-connected with the DMN. The aPFC is proposed to play a major role in the highest level of integration of information received from visual, auditory, and somatic sensory systems to achieve amodal, abstract, conceptual interpretation of the environment (Christoff et al., 2003; Petrides & Pandya, 2007). The aPFC may also play a role in influencing abstract information processing and the integration of the outcomes of multiple cognitive operations (Ramnani & Owen, 2004). Thus, poor intra-DMN Fc of aPFC may relate to the deficits in abstracting abilities and sensory processing in ASD. Typically, the medial aspect of aPFC is functionally and anatomically connected with the major DMN regions of the mPFC, PCC, and lateral parietal cortex (Liu et al., 2013). Whether the reduced functional connectivity of the DMN with aPFC in the ASD sample of this study can be corroborated with aberrant structural connectivity remains to be investigated.

The AG is a functionally heterogeneous region typically involved in semantic processing bilaterally and, as a component of Rt. TPJ (rTPJ) in conjunction with the SMG, is engaged in attention processing (Decety & Lamm, 2007; Igelstrom et al., 2015; Kubit & Jack, 2013; Scholz et al., 2009). Recent functional neuroimaging literature suggests impaired functioning of Rt. AG in ASD correlates with severity of inattention and social deficits (Redcay et al., 2013; You et al., 2013). Additionally, reduced RsFc of the Lt. AG in ASD inversely correlates with autism severity (Kennedy & Courchesne, 2008; von dem Hagen et al., 2013). Hence, our finding of reduced integration of Bl. AG with the DMN is consistent with the prevailing literature.

Segregation of DMN in ASD (Negative-correlations)

In addition to poor integration of the DMN in ASD, there was evidence of poor functional segregation with the TP regions in the Rt. hemisphere. The typically expected correlational directionality of the extra-DMN connectivity with TP regions in the Rt. hemisphere was inversed from negative to positive, suggesting that instead of being suppressed, certain anti-correlated regions are co-activated with DMN in ASD. Positive correlations reflect an integrative role in combining neuronal activity sub-serving similar functions whereas anti-correlations signify segregation of neuronal processes that sub-serve opposite functions or competing representations. Furthermore, the ability to switch between DMN and TP network relies on the strength of anti-correlations between these two networks that facilitates toggling between competing introspective and extrospective attentional demands (Broyd et al., 2009). Based on this understanding, one could speculate that our findings of the lack of anti-correlations and atypical linkage of TP-regions with the DMN may reflect a functional failure of TP network deactivation and aberrant activation, consequently altering the functional relationship between the DMN and TP networks in ASD. This may clinically translate as compromised self-referential processing and impaired ability to switch between introspective and extrospective neural processes.

The RsFc of the DMN with the FG was atypical in ASD. The lateral aspect of Rt. FG exhibited atypical functional integration with the DMN. The nature of the DMN RsFc with lateral FG and aVC brain region, which is typically segregating (Fox et al., 2005), was paradoxically integrating in ASD. The FG has been the subject of previously identified abnormality in brain imaging studies of autism (Corbett et al., 2009; Pierce & Redcay, 2008). Hypo-activation and reduced Fc of the FG to frontal regions has been reported in autism during facial processing tasks (Critchley et al., 2000; Kleinhans et al., 2008; Koshino et al., 2008; Pierce et al., 2001; Schultz et al., 2000). Thus, atypical Fc of the Rt. lateral FG/aVC may relate to poor attention to facial expressions and non-verbal communication deficits observed in ASD.

In this study, the DMN in ASD was atypically correlated with the Rt. hemispheric regions of AG, SMG, pSTG. Taken together, these regions constitute the rTPJ, which plays a critical role in processing social cognition, empathy, and reorienting attention (Decety &

Brain Connectivity
Integration and Segregation of Default Mode Network Resting-state Functional Connectivity in Transition-age Males with High-functioning Autism Spectrum Disorder: A Proof of Concept Study (DOI: 10.1089/brain.2016.0483)
This paper has been peer-reviewed and accepted for publication, but has yet to undergo copyediting and proof correction. The final published version may differ from this proof.

Lamm, 2007; Kubit & Jack, 2013). Abnormal functional activity of TPJ has been documented in individuals with ASD during social task-related activity (Di Martino et al., 2009) or at rest (Anderson et al., 2011b; Fishman et al., 2014; Igelstrom et al., 2016; Lai et al., 2010; Mueller et al., 2013; von dem Hagen et al., 2013). Consistent with our findings, abnormal functional activity of rTPJ and its connectivity is increasingly being implicated in the pathophysiology of ASD (Igelstrom et al., 2016; Mueller et al., 2013; Pantelis et al., 2015; von dem Hagen et al., 2013).

The DMN in ASD, as opposed to in HC, was positively correlated with the Rt. SMG. As functional components of rTPJ, the SMG is typically recruited for reorienting and maintaining attention on externally-oriented non-social tasks and the AG is functionally engaged in social cognitive processes. Typically, SMG and AG as part of rTPJ share anti-correlated patterns of RsFc, which reflect the opposing nature of their functional relationship. For example, non-social task-based activation of SMG (as part of TP network activation) suppresses AG, which in turn deactivates the DMN. Thus, our results suggesting lack of anti-correlation between SMG and DMN in ASD may have bearing on the ability of the rTPJ to suppress DMN during TP activity. Additionally, atypical integration of the DMN with SMG in ASD suggests interfering activation of TP regions during introspective and social-emotion activity. Previous studies in ASD have reported SMG impairments in the context of social skill impairments (Abrams, et al., 2013; Salmi, et al., 2013). Failure to suppress the DMN during TP activation may also present as poor reorienting ability and attentional difficulties that are often associated with ASD. Specifically, activation of SMG during DMN activity may adversely affect social-emotion processing and performance in individuals with ASD.

The ABIDE dataset analysis revealed a significant lack of anti-correlation between DMN and the Rt. hemispheric regions of SMG and pSTG. In addition, significant correlation was observed between the strength of anti-correlation between DMN and Rt. SMG/pSTG and the severity of autism on the ADOS (total score). Specifically, reductions in anti-correlations corresponded positively with symptom severity. This further highlights the importance of examining the anti-correlations in the study of DMN in ASD.

Pattern Recognition Performance in ASD

A wide variability was observed in the RsFc strength of mean DMN seed to ROIs that survived between-group second-level DMN analysis suggesting heterogeneity in RsFc neural profile in ASD. This heterogeneity was further emphasized in the clustering analysis that noted presence of sub-groups with distinct neural profiles. The neural heterogeneity with ASD observed in this study is consistent with the heterogeneous phenotypic expression of ASD.

Remarkably, all the ROIs that survived the second-level between-group DMN analysis belonged to either task-negative i.e., DMN (mPFC, Bl. AG, Lt. cerebellar lobule) or TP network (Rt. Hemispheric FG, VC, SMG, pSTG, AC). On further assessment of these nine regions that survived the second-level between-group significance tests, we found that the inter-connectivity between these regions was significantly weaker in the ASD subjects. Thus, the nine identified ROIs not only differed in their connectivity with the DMN but in their connectivity with each other. Furthermore, by inspecting the MSTs, we could probe differences in the topology of the ROI connections between the HC and ASD subjects. We defined two types of ROIs based on their connectivity with the DMN; six positively correlated and three negatively correlated ROIs. The MSTs revealed that in HCs the two types of ROIs were more tightly connected within their own types; while in ASD this pattern seems to be disrupted, as observed by the intermixing of the two types of ROIs (Figure-V.B). The atypical MST topology (characterized by anti-correlated TP regions integrated with the TN DMN regions) was more frequently present in ASD (67%) than HC (6%) participants. Our results suggest that the topology of the connections, in addition to the connection strengths, can potentially serve as a marker for identification and quantification of ASD. We speculate that such analysis of the topology of connections between brain regions could pave a way for identifying neural markers for the diagnosis of ASD.

Limitations

Our study involved a small sample of intellectually capable Caucasian males with ASD and co-occurring psychiatric conditions. Although non-parametric approaches are ideal for accounting for false positives, we resorted to standard parametric approaches because of

our small sample size. Since previous studies have proven the test-retest reproducibility of DMN at 3 Tesla (Meindl et al., 2010) with a small sample size (N=18) we have limited our explorations to DMN. Alterations in the DMN are observed with various neuropsychiatric disorders including ADHD, mood disorders, and schizophrenia (Castellanos et al., 2008; Drevets et al., 2008; Garrity et al., 2007; Greicius et al., 2007). More detailed studies are needed to identify disorder-specific changes in the DMN. The impact of comorbidity and associated medication treatment might be potential confounds. Although the age range of the ASD participants represents transition age individuals, our findings remain subject to brain developmental related differences. Employing superior spatial resolution in this study without compromising on whole-brain coverage resulted in a lower temporal resolution, and therefore a low number of total time points per subject. Employing simultaneous multi-slice imaging techniques in future studies would avoid such limitations (as evident from the ABIDE sample) and provide statistical power enhancements (Setsompop et al., 2012) and rigorous execution of denoising strategies. Furthermore, we recognize that the clustering and MST results would be more informative with a larger sample. Nonetheless, our current novel analysis paves the way for new methodologies. We speculate that MST topology, identified using correlations and anti-correlations between ROIs, can reveal additional information about individual differences in ASD; we leave this for future research.

Conclusions

Despite these limitations, results of this study highlight that the RsFc profile of the DMN in transition-age males with HF-ASD was atypically characterized by reduced integration and lack of segregation from regions that typically belong to the TP network. In addition, this study offered proof of concept on the applicability of pattern recognition analysis techniques for identifying sub-clusters that share distinct profiles of DMN RsFc with brain regions of interest, and for mapping the individual MST profiles of the inter-ROI RsFc relationship between the DMN and TP network regions identified in this study as atypical in ASD. The preliminary findings of an atypical RsFc profile of the DMN in ASD as identified in this pilot study hold the potential to serve as diagnostic neural markers and warrant future investigation in larger samples of the ASD population.

Acknowledgements:

This work is funded in part by the Alan and Lorraine Bressler Clinical and Research Program for Autism Spectrum Disorder, the Saylor Family Fund for Autism Research, the MGH Pediatric Psychopharmacology Council Fund, and by the National Institute of Mental Health grant awarded to Gagan Joshi (#K23MH100450). Imaging was performed at the Athinoula A. Martinos Imaging Center at the McGovern Institute for Brain Research, Massachusetts Institute of Technology.

Brain Connectivity
Integration and Segregation of Default Mode Network Resting-state Functional Connectivity in Transition-age Males with High-functioning Autism Spectrum Disorder: A Proof of Concept Study (DOI: 10.1089/brain.2016.0483)
This paper has been peer-reviewed and accepted for publication, but has yet to undergo copyediting and proof correction. The final published version may differ from this proof.

REFERENCES

Abrams, D.A., Lynch, C.J., Cheng, K.M., Phillips, J., Supekar, K., Ryali, S., Uddin, L.Q., Menon, V. (2013) Underconnectivity between voice-selective cortex and reward circuitry in children with autism. Proceedings of the National Academy of Sciences of the United States of America, 110:12060-5.

Adolphs, R. (2009) The social brain: neural basis of social knowledge. Annual review of psychology, 60:693-716.

American Psychiatric Association. (1987). Diagnostic and statis- tical manual of mental disorders (3rd ed., Rev.). Washington, DC: Author.

American Psychiatric Association. (1994). Diagnostic and statis- tical manual of mental disorders (4th ed.). Washington, DC: Author.

American Psychiatric Association. Diagnostic and statistical manual of mental disorders. 5th ed. Arlington, VA: American Psychiatric Association; 2013

Anderson, J.S., Druzgal, T.J., Lopez-Larson, M., Jeong, E.K., Desai, K., Yurgelun-Todd, D. (2011a) Network anticorrelations, global regression, and phase-shifted soft tissue correction. Human brain mapping, 32:919-34.

Anderson, J.S., Nielsen, J.A., Froehlich, A.L., DuBray, M.B., Druzgal, T.J., Cariello, A.N., Cooperrider, J.R., Zielinski, B.A., Ravichandran, C., Fletcher, P.T., Alexander, A.L., Bigler, E.D., Lange, N., Lainhart, J.E. (2011b) Functional connectivity magnetic resonance imaging classification of autism. Brain : a journal of neurology, 134:3742-54.

Ashburner, J., Friston, K.J. (2005) Unified segmentation. NeuroImage, 26:839-51.

Assaf, M., Jagannathan, K., Calhoun, V.D., Miller, L., Stevens, M.C., Sahl, R., O'Boyle, J.G., Schultz, R.T., Pearlson, G.D. (2010) Abnormal functional connectivity of default mode sub-networks in autism spectrum disorder patients. NeuroImage, 53:247-56.

Barttfeld, P., Wicker, B., Cukier, S., Navarta, S., Lew, S., Leiguarda, R., Sigman, M. (2012) State-dependent changes of connectivity patterns and functional brain network topology in autism spectrum disorder. Neuropsychologia, 50:3653-62.

Behzadi, Y., Restom, K., Liau, J., Liu, T.T. (2007) A component based noise correction method (CompCor) for BOLD and perfusion based fMRI. Neuroimage, 37:90-101.

Ben Shalom, D., Mostofsky, S.H., Hazlett, R.L., Goldberg, M.C., Landa, R.J., Faran, Y., McLeod, D.R., Hoehn-Saric, R. (2006) Normal physiological emotions but differences in expression of conscious feelings in children with high-functioning autism. Journal of autism and developmental disorders, 36:395-400.

Berument SK, Rutter M, Lord C et al (1999) Autism screening questionnaire: diagnostic validity. Br J Psychiatry 175:444–451.

Biswal, B., Yetkin, F.Z., Haughton, V.M., Hyde, J.S. (1995) Functional connectivity in the motor cortex of resting human brain using echo-planar MRI. Magnetic resonance in medicine, 34:537-41.

Blakemore, S.J. (2008) The social brain in adolescence. Nature reviews. Neuroscience, 9:267-77.

Blakemore, S.J., Choudhury, S. (2006) Development of the adolescent brain: implications for executive function and social cognition. Journal of child psychology and psychiatry, and allied disciplines, 47:296-312.

Blumberg SJ, Bramlett MD, Kogan MD, et al. Changes in prevalence of parent-reported autism spectrum disorder in school-aged U.S. children: 2007 to 2011–2012. Natl Health Stat Report. 2013:1–11.

Broyd, S.J., Demanuele, C., Debener, S., Helps, S.K., James, C.J., Sonuga-Barke, E.J. (2009) Default-mode brain dysfunction in mental disorders: a systematic review. Neuroscience and biobehavioral reviews, 33:279-96.

Buckner, R.L., Andrews-Hanna, J.R., Schacter, D.L. (2008) The brain's default network: anatomy, function, and relevance to disease. Annals of the New York Academy of Sciences, 1124:1-38.

Calhoun, V.D., Adali, T., Pearlson, G.D., Pekar, J.J. (2001) A method for making group inferences from functional MRI data using independent component analysis. Human brain mapping, 14:140-51.

Caspers S, Geyer S, Schleicher A, Mohlberg H, Amunts K, Zilles K. 2006. The human inferior parietal cortex: cytoarchitectonic parcellation and interindividual variability. Neuroimage. 33:430--448.

Castellanos, F.X., Margulies, D.S., Kelly, C., Uddin, L.Q., Ghaffari, M., Kirsch, A., Shaw, D., Shehzad, Z., Di Martino, A., Biswal, B., Sonuga-Barke, E.J., Rotrosen, J., Adler, L.A.,

Milham, M.P. (2008) Cingulate-precuneus interactions: a new locus of dysfunction in adult attention-deficit/hyperactivity disorder. Biological psychiatry, 63:332-7.

Chai, X.J., Castanon, A.N., Ongur, D., Whitfield-Gabrieli, S. (2012) Anticorrelations in resting state networks without global signal regression. NeuroImage, 59:1420-8.

Chambers, W. J., Puig-Antich, J., Hirsch, M., Paez, P., Ambrosini, P. J., Tabrizi, M. A., et al. (1985). The assessment of affective disorders in children and adolescents by semistructured inter- view. Test-retest reliability of the schedule for affective disor- ders and schizophrenia for school-age children, present episode version. Archives of General Psychiatry, 42(7), 696–702.

Christoff, K., Ream, J.M., Geddes, L.P., Gabrieli, J.D. (2003) Evaluating self-generated information: anterior prefrontal contributions to human cognition. Behavioral neuroscience, 117:1161-8.

Corbett, B.A., Carmean, V., Ravizza, S., Wendelken, C., Henry, M.L., Carter, C., Rivera, S.M. (2009) A functional and structural study of emotion and face processing in children with autism. Psychiatry research, 173:196-205.

Critchley, H.D., Daly, E.M., Bullmore, E.T., Williams, S.C., Van Amelsvoort, T., Robertson, D.M., Rowe, A., Phillips, M., McAlonan, G., Howlin, P., Murphy, D.G. (2000) The functional neuroanatomy of social behaviour: changes in cerebral blood flow when people with autistic disorder process facial expressions. Brain : a journal of neurology, 123 (Pt 11):2203-12.

Decety, J., Lamm, C. (2007) The role of the right temporoparietal junction in social interaction: how low-level computational processes contribute to meta-cognition. The Neuroscientist : a review journal bringing neurobiology, neurology and psychiatry, 13:580-93.

Di Martino, A., Ross, K., Uddin, L.Q., Sklar, A.B., Castellanos, F.X., Milham, M.P. (2009) Functional brain correlates of social and nonsocial processes in autism spectrum disorders: an activation likelihood estimation meta-analysis. Biological psychiatry, 65:63-74.

Di Martino, A., Zuo, X.N., Kelly, C., Grzadzinski, R., Mennes, M., Schvarcz, A., Rodman, J., Lord, C., Castellanos, F.X., Milham, M.P. (2013) Shared and distinct intrinsic

functional network centrality in autism and attention-deficit/hyperactivity disorder. Biological psychiatry, 74:623-32.

Dosenbach, N.U., Nardos, B., Cohen, A.L., Fair, D.A., Power, J.D., Church, J.A., Nelson, S.M., Wig, G.S., Vogel, A.C., Lessov-Schlaggar, C.N., Barnes, K.A., Dubis, J.W., Feczko, E., Coalson, R.S., Pruett, J.R., Jr., Barch, D.M., Petersen, S.E., Schlaggar, B.L. (2010) Prediction of individual brain maturity using fMRI. Science, 329:1358-61.

Drevets, W.C., Savitz, J., Trimble, M. (2008) The subgenual anterior cingulate cortex in mood disorders. CNS spectrums, 13:663-81.

Ebisch, S.J., Gallese, V., Willems, R.M., Mantini, D., Groen, W.B., Romani, G.L., Buitelaar, J.K., Bekkering, H. (2011) Altered intrinsic functional connectivity of anterior and posterior insula regions in high-functioning participants with autism spectrum disorder. Human brain mapping, 32:1013-28.

Eilam-Stock, T., Xu, P., Cao, M., Gu, X., Van Dam, N.T., Anagnostou, E., Kolevzon, A., Soorya, L., Park, Y., Siller, M., He, Y., Hof, P.R., Fan, J. (2014) Abnormal autonomic and associated brain activities during rest in autism spectrum disorder. Brain : a journal of neurology, 137:153-71.

First, M., Gibbon, M., Williams, J., & Spitzer, R. (1996). Structured clinical interview for DSM-IV disorders: SCID SCREEN Patient Questionnaire Computer Program. Washington, DC: American Psychiatric Press.

Fishman, I., Keown, C.L., Lincoln, A.J., Pineda, J.A., Muller, R.A. (2014) Atypical cross talk between mentalizing and mirror neuron networks in autism spectrum disorder. JAMA psychiatry, 71:751-60.

Fox, M.D., Snyder, A.Z., Vincent, J.L., Corbetta, M., Van Essen, D.C., Raichle, M.E. (2005) The human brain is intrinsically organized into dynamic, anticorrelated functional networks. Proceedings of the National Academy of Sciences of the United States of America, 102:9673-8.

Fraley, C., Raftery, A.E. (2012) mclust Version 4 for R: Normal Mixture Modeling for Model-Based Clustering, Classification, and Density Estimation. Technical Report No. 597. Department of Statistics, University of Washington. https://www.stat.washington.edu/research/reports/2012/tr597.pdf

Frith, C.D., Frith, U. (2007) Social cognition in humans. Current biology : CB, 17:R724-32.

Frith, U., Frith, C.D. (2003) Development and neurophysiology of mentalizing. Philosophical transactions of the Royal Society of London. Series B, Biological sciences, 358:459-73.

Garrity, A.G., Pearlson, G.D., McKiernan, K., Lloyd, D., Kiehl, K.A., Calhoun, V.D. (2007) Aberrant "default mode" functional connectivity in schizophrenia. The American journal of psychiatry, 164:450-7.

Greicius, M.D., Flores, B.H., Menon, V., Glover, G.H., Solvason, H.B., Kenna, H., Reiss, A.L., Schatzberg, A.F. (2007) Resting-state functional connectivity in major depression: abnormally increased contributions from subgenual cingulate cortex and thalamus. Biological psychiatry, 62:429-37.

Greicius, M.D., Krasnow, B., Reiss, A.L., Menon, V. (2003) Functional connectivity in the resting brain: a network analysis of the default mode hypothesis. Proceedings of the National Academy of Sciences of the United States of America, 100:253-8.

Hill, E., Berthoz, S., Frith, U. (2004) Brief report: cognitive processing of own emotions in individuals with autistic spectrum disorder and in their relatives. Journal of autism and developmental disorders, 34:229-35.

Hollingshead, A. B. (1975). Four factor index of social status. New Haven, CT: Yale Press.

Igelstrom, K.M., Webb, T.W., Graziano, M.S. (2015) Neural Processes in the Human Temporoparietal Cortex Separated by Localized Independent Component Analysis. The Journal of neuroscience : the official journal of the Society for Neuroscience, 35:9432-45.

Johnson, S.C., Baxter, L.C., Wilder, L.S., Pipe, J.G., Heiserman, J.E., Prigatano, G.P. (2002) Neural correlates of self-reflection. Brain : a journal of neurology, 125:1808-14.

Jolliffe, I.T. (2002). Principal Component Analysis. Springer Series in Statistics.

Kennedy, D.P., Courchesne, E. (2008) Functional abnormalities of the default network during self- and other-reflection in autism. Social cognitive and affective neuroscience, 3:177-90.

Kleinhans, N.M., Richards, T., Sterling, L., Stegbauer, K.C., Mahurin, R., Johnson, L.C., Greenson, J., Dawson, G., Aylward, E. (2008) Abnormal functional connectivity in autism spectrum disorders during face processing. Brain : a journal of neurology, 131:1000-12.

Koshino, H., Kana, R.K., Keller, T.A., Cherkassky, V.L., Minshew, N.J., Just, M.A. (2008) fMRI investigation of working memory for faces in autism: visual coding and underconnectivity with frontal areas. Cerebral cortex, 18:289-300.

Kubit, B., Jack, A.I. (2013) Rethinking the role of the rTPJ in attention and social cognition in light of the opposing domains hypothesis: findings from an ALE-based meta-analysis and resting-state functional connectivity. Frontiers in human neuroscience, 7:323.

Lai, M.C., Lombardo, M.V., Chakrabarti, B., Sadek, S.A., Pasco, G., Wheelwright, S.J., Bullmore, E.T., Baron-Cohen, S., Consortium, M.A., Suckling, J. (2010) A shift to randomness of brain oscillations in people with autism. Biological psychiatry, 68:1092-9.

Liu, H., Qin, W., Li, W., Fan, L., Wang, J., Jiang, T., Yu, C. (2013) Connectivity-based parcellation of the human frontal pole with diffusion tensor imaging. The Journal of neuroscience : the official journal of the Society for Neuroscience, 33:6782-90.

Lowe, M.J., Dzemidzic, M., Lurito, J.T., Mathews, V.P., Phillips, M.D. (2000) Correlations in low-frequency BOLD fluctuations reflect cortico-cortical connections. NeuroImage, 12:582-7.

Lynch, C.J., Uddin, L.Q., Supekar, K., Khouzam, A., Phillips, J., Menon, V. (2013) Default mode network in childhood autism: posteromedial cortex heterogeneity and relationship with social deficits. Biological psychiatry, 74:212-9.

Maldjian, J.A., Laurienti, P.J., Kraft, R.A., Burdette, J.H. (2003) An automated method for neuroanatomic and cytoarchitectonic atlas-based interrogation of fMRI data sets. NeuroImage, 19:1233-9.

Meindl, T., Teipel, S., Elmouden, R., Mueller, S., Koch, W., Dietrich, O., Coates, U., Reiser, M., Glaser, C. (2010) Test-retest reproducibility of the default-mode network in healthy individuals. Human brain mapping, 31:237-46.

Mitchell, J.P. (2009) Social psychology as a natural kind. Trends in cognitive sciences, 13:246-51.

Monk, C.S., Peltier, S.J., Wiggins, J.L., Weng, S.J., Carrasco, M., Risi, S., Lord, C. (2009) Abnormalities of intrinsic functional connectivity in autism spectrum disorders. NeuroImage, 47:764-72.

Mueller, S., Keeser, D., Samson, A.C., Kirsch, V., Blautzik, J., Grothe, M., Erat, O., Hegenloh, M., Coates, U., Reiser, M.F., Hennig-Fast, K., Meindl, T. (2013) Convergent Findings of Altered Functional and Structural Brain Connectivity in Individuals with High Functioning Autism: A Multimodal MRI Study. PloS one, 8:e67329.

Muller, R.A., Shih, P., Keehn, B., Deyoe, J.R., Leyden, K.M., Shukla, D.K. (2011) Underconnected, but how? A survey of functional connectivity MRI studies in autism spectrum disorders. Cerebral cortex, 21:2233-43.

Murphy, K., Birn, R.M., Handwerker, D.A., Jones, T.B., Bandettini, P.A. (2009) The impact of global signal regression on resting state correlations: are anti-correlated networks introduced? NeuroImage, 44:893-905.

Nicolson, R., Szatmari, P. (2003) Genetic and neurodevelopmental influences in autistic disorder. Canadian journal of psychiatry. Revue canadienne de psychiatrie, 48:526-37.

Ochsner, K.N., Beer, J.S., Robertson, E.R., Cooper, J.C., Gabrieli, J.D., Kihsltrom, J.F., D'Esposito, M. (2005) The neural correlates of direct and reflected self-knowledge. NeuroImage, 28:797-814.

Oldfield, R.C. (1971) The assessment and analysis of handedness: the Edinburgh inventory. Neuropsychologia, 9:97-113.

Olson, I.R., Plotzker, A., Ezzyat, Y. (2007) The Enigmatic temporal pole: a review of findings on social and emotional processing. Brain : a journal of neurology, 130:1718-31.

Orvaschel, H. (1994). Schedule for Affective Disorders and Schizophrenia for School-Age Children Epidemiologic Version (5th ed.). Fort Lauderdale, FL: Nova Southeastern University, Center for Psychological Studies.

Orvaschel, H., & Puig-Antich, J. (1987). Schedule for Affective Disorders and Schizophrenia for School-Age Children: Epidemiologic Version. Fort Lauderdale, FL: Nova University.

Pantelis, P.C., Byrge, L., Tyszka, J.M., Adolphs, R., Kennedy, D.P. (2015) A specific hypoactivation of right temporo-parietal junction/posterior superior temporal sulcus in response to socially awkward situations in autism. Social cognitive and affective neuroscience, 10:1348-56.

Petrides, M., Pandya, D.N. (2007) Efferent association pathways from the rostral prefrontal cortex in the macaque monkey. The Journal of neuroscience : the official journal of the Society for Neuroscience, 27:11573-86.

Pierce, K., Muller, R.A., Ambrose, J., Allen, G., Courchesne, E. (2001) Face processing occurs outside the fusiform 'face area' in autism: evidence from functional MRI. Brain : a journal of neurology, 124:2059-73.

Pierce, K., Redcay, E. (2008) Fusiform function in children with an autism spectrum disorder is a matter of "who". Biological psychiatry, 64:552-60.

R Core Team (2015). R: A language and environment for statistical computing. R Foundatio n for

Statistical Computing, Vienna, Austria. URL http://www.R-project.org/.

Raichle, M.E. (2011) The restless brain. Brain Connect, 1:3-12.

Raichle, M.E., Gusnard, D.A. (2005) Intrinsic brain activity sets the stage for expression of motivated behavior. The Journal of comparative neurology, 493:167-76.

Raichle, M.E., MacLeod, A.M., Snyder, A.Z., Powers, W.J., Gusnard, D.A., Shulman, G.L. (2001) A default mode of brain function. Proceedings of the National Academy of Sciences of the United States of America, 98:676-82.

Ramnani, N., Owen, A.M. (2004) Anterior prefrontal cortex: insights into function from anatomy and neuroimaging. Nature reviews. Neuroscience, 5:184-94.

Redcay, E., Moran, J.M., Mavros, P.L., Tager-Flusberg, H., Gabrieli, J.D., Whitfield-Gabrieli, S. (2013) Intrinsic functional network organization in high-functioning adolescents with autism spectrum disorder. Frontiers in human neuroscience, 7:573.

Rieffe, C., Meerum Terwogt, M., Kotronopoulou, K. (2007) Awareness of single and multiple emotions in high-functioning children with autism. Journal of autism and developmental disorders, 37:455-65.

Rudie, J.D., Shehzad, Z., Hernandez, L.M., Colich, N.L., Bookheimer, S.Y., Iacoboni, M., Dapretto, M. (2012) Reduced functional integration and segregation of distributed neural systems underlying social and emotional information processing in autism spectrum disorders. Cerebral cortex, 22:1025-37.

Rutter M, Bailey A, Lord C (2003) Social communication questionnaire. Western Psychological Services, Los Angeles.

Salmi, J., Roine, U., Glerean, E., Lahnakoski, J., Nieminen-von Wendt, T., Tani, P., Leppamaki, S., Nummenmaa, L., Jaaskelainen, I.P., Carlson, S., Rintahaka, P., Sams, M. (2013) The brains of high functioning autistic individuals do not synchronize with those of others. NeuroImage. Clinical, 3:489-97.

Scholz, J., Triantafyllou, C., Whitfield-Gabrieli, S., Brown, E.N., Saxe, R. (2009) Distinct regions of right temporo-parietal junction are selective for theory of mind and exogenous attention. PloS one, 4:e4869.

Schultz, R.T., Gauthier, I., Klin, A., Fulbright, R.K., Anderson, A.W., Volkmar, F., Skudlarski, P., Lacadie, C., Cohen, D.J., Gore, J.C. (2000) Abnormal ventral temporal cortical activity during face discrimination among individuals with autism and Asperger syndrome. Archives of general psychiatry, 57:331-40.

Seeley, W.W., Crawford, R.K., Zhou, J., Miller, B.L., Greicius, M.D. (2009) Neurodegenerative diseases target large-scale human brain networks. Neuron, 62:42-52.

Setsompop, K., Gagoski, B.A., Polimeni, J.R., Witzel, T., Wedeen, V.J., Wald, L.L. (2012) Blipped-controlled aliasing in parallel imaging for simultaneous multislice echo planar imaging with reduced g-factor penalty. Magnetic resonance in medicine, 67:1210-24.

Sherman, L.E., Rudie, J.D., Pfeifer, J.H., Masten, C.L., McNealy, K., Dapretto, M. (2014) Development of the default mode and central executive networks across early adolescence: a longitudinal study. Developmental cognitive neuroscience, 10:148-59.

Stam, C.J. (2014) Modern network science of neurological disorders. Nature reviews. Neuroscience, 15:683-95.

Starck, T., Nikkinen, J., Rahko, J., Remes, J., Hurtig, T., Haapsamo, H., Jussila, K., Kuusikko-Gauffin, S., Mattila, M.L., Jansson-Verkasalo, E., Pauls, D.L., Ebeling, H., Moilanen, I., Tervonen, O., Kiviniemi, V.J. (2013) Resting state fMRI reveals a default mode

dissociation between retrosplenial and medial prefrontal subnetworks in ASD despite motion scrubbing. Frontiers in human neuroscience, 7:802.

Tewarie, P., van Dellen, E., Hillebrand, A., Stam, C.J. (2015) The minimum spanning tree: an unbiased method for brain network analysis. NeuroImage, 104:177-88.

Thesen, S., Heid, O., Mueller, E., Schad, L.R. (2000) Prospective acquisition correction for head motion with image-based tracking for real-time fMRI. Magnetic resonance in medicine, 44:457-65.

Uddin, L.Q. (2011) The self in autism: an emerging view from neuroimaging. Neurocase, 17:201-8.

Uddin LQ, Supekar K, Amin H, Rykhlevskaia E, Nguyen DA, Greicius MD, Menon V. Dissociable connectivity within human angular gyrus and intraparietal sulcus: evidence from functional and structural connectivity. Cereb Cortex. 2010 Nov;20(11):2636-46.

Uddin, L.Q., Supekar, K., Menon, V. (2013) Reconceptualizing functional brain connectivity in autism from a developmental perspective. Frontiers in human neuroscience, 7:458.

von dem Hagen, E.A., Stoyanova, R.S., Baron-Cohen, S., Calder, A.J. (2013) Reduced functional connectivity within and between 'social' resting state networks in autism spectrum conditions. Social cognitive and affective neuroscience, 8:694-701.

Washington, S.D., Gordon, E.M., Brar, J., Warburton, S., Sawyer, A.T., Wolfe, A., Mease-Ference, E.R., Girton, L., Hailu, A., Mbwana, J., Gaillard, W.D., Kalbfleisch, M.L., VanMeter, J.W. (2014) Dysmaturation of the default mode network in autism. Human brain mapping, 35:1284-96.

Weng, S.J., Wiggins, J.L., Peltier, S.J., Carrasco, M., Risi, S., Lord, C., Monk, C.S. (2010) Alterations of resting state functional connectivity in the default network in adolescents with autism spectrum disorders. Brain research, 1313:202-14.

Whitfield-Gabrieli, S., Moran, J.M., Nieto-Castanon, A., Triantafyllou, C., Saxe, R., Gabrieli, J.D. (2011) Associations and dissociations between default and self-reference networks in the human brain. NeuroImage, 55:225-32.

Whitfield-Gabrieli, S., Nieto-Castanon, A. (2012) Conn: a functional connectivity toolbox for correlated and anticorrelated brain networks. Brain Connect, 2:125-41.

Wiggins, J.L., Peltier, S.J., Ashinoff, S., Weng, S.J., Carrasco, M., Welsh, R.C., Lord, C., Monk, C.S. (2011) Using a self-organizing map algorithm to detect age-related changes in functional connectivity during rest in autism spectrum disorders. Brain research, 1380:187-97.

You, X., Norr, M., Murphy, E., Kuschner, E.S., Bal, E., Gaillard, W.D., Kenworthy, L., Vaidya, C.J. (2013) Atypical modulation of distant functional connectivity by cognitive state in children with Autism Spectrum Disorders. Frontiers in human neuroscience, 7:482.

Zhao, F., Qiao, L., Shi, F., Yap, P.T., Shen, D. (2016) Feature fusion via hierarchical supervised local CCA for diagnosis of autism spectrum disorder. Brain imaging and behavior.

Brain Connectivity
Integration and Segregation of Default Mode Network Resting-state Functional Connectivity in Transition-age Males with High-functioning Autism Spectrum Disorder: A Proof of Concept Study (DOI: 10.1089/brain.2016.0483)
This paper has been peer-reviewed and accepted for publication, but has yet to undergo copyediting and proof correction. The final published version may differ from this proof.

Abbreviations

aCompcor: anatomical Component based noise Correction

ADHD: Attention-deficit/hyperactivity disorder

APA: American Psychiatric Association

ASD: Autism Spectrum Disorder

BIC: Bayesian Information Criterion

BOLD: Blood Oxygen Level Dependent

DMN: Default Mode Network

DSM: Diagnostic and Statistical Manual of Mental Disorders

EPI: Echo Planar Imaging

fMRI: functional Magnetic Resonance Imaging

GSR: Global Signal Regression

GMM: Gaussian mixture modeling

HC: Healthy Controls

ICA: Independent Component Analyses

IQ: Intelligence Quotient

K-SADS-E: Kiddie Schedule for Affective Disorders and Schizophrenia-Epidemiological Version

MST: Minimum Spanning Tree

PACE: Prospective Acquisition CorrEction

PCA: Principal Component Analyses

ROI: Region of Interest

RsFc: Resting-state Functional connectivity

SCID: Structured Clinical Interview for DSM-IV

TN: Task Positive

ToM: Theory of Mind

TP: Task Negative

Brain Connectivity
Integration and Segregation of Default Mode Network Resting-state Functional Connectivity in Transition-age Males with High-functioning Autism Spectrum Disorder: A Proof of Concept Study (DOI: 10.1089/brain.2016.0483)
This paper has been peer-reviewed and accepted for publication, but has yet to undergo copyediting and proof correction. The final published version may differ from this proof.

Table-I A *priori* Literature-based* DMN seeds of interest

DMN Seeds of Interest [Cluster Size=5mm^3]	**BA**	**MNI** [x, y, z]
Medial Pre-frontal Cortex	32/10	+00 +48 -04
Posterior Cingulate Cortex/Precuneus	31/7	-06 -52 +40
Bilateral Posterior Angular Gyrus	39	±46 -70 +36
Bilateral Inferior Temporal Gyrus	21	+58/-61 -24 -09

BA=Brodmann area; MNI=Montreal Neurologic Institute

*Fox et al., 2005 & Raichle, 2011

Brain Connectivity
Integration and Segregation of Default Mode Network Resting-state Functional Connectivity in Transition-age Males with High-functioning Autism Spectrum Disorder: A Proof of Concept Study (DOI: 10.1089/brain.2016.0483)
This paper has been peer-reviewed and accepted for publication, but has yet to undergo copyediting and proof correction. The final published version may differ from this proof.

Table-II Demographics & Clinical Characteristics

	ASD	**HC**	**p-value**
Demographics			
Total Participants	15	16	
Age *(years)*			
Mean (Range)	21.6 ±3.7 (16-28)	21.9 ±3.5 (15-29)	p=0.82
<18 years	3 (20)	1 (6)	
Gender: Male	15 (100)	16 (100)	
Race: Caucasian	14 (93)	8 (50)	p=0.02
Handedness: Right-handed	14 (93)	15 (94)	
Socioeconomic status* *(Class 4 or 5)*	1 (6)	U/A	
Full Scale IQ (Range)	111 ±10 (96-130)	123 ±9.2 (105-138)	p=0.001
Clinical Characteristics			
ASD Subtypes			
Autistic disorder	10 (67)	N/A	
Asperger's disorder	3 (20)	N/A	
PDD-NOS	2 (13)	N/A	
ASD Impairment *(Lifetime; N=14)*			
Mild	0 (0)	N/A	
Moderate	10 (71.4)	N/A	

Severe	04 (28.6)	N/A

Values expressed as N (%) or Mean ±Standard Deviation; HC= Healthy Controls; ASD=Autism Spectrum Disorder; IQ=Intelligence Quotient; PDD-NOS=Pervasive Developmental Disorder Not Otherwise Specified; N/A=Not Applicable; U/A=Unavailable; *Four Factor Index of Social Status

Brain Connectivity
Integration and Segregation of Default Mode Network Resting-state Functional Connectivity in Transition-age Males with High-functioning Autism Spectrum Disorder: A Proof of Concept Study (doi: 10.1089/brain.2016.0483)
This paper has been peer-reviewed and accepted for publication, but has yet to undergo copyediting and proof correction. The final published version may differ from this proof.

Brain Connectivity
Integration and Segregation of Default Mode Network Resting-state Functional Connectivity in Transition-age Males with High-functioning Autism Spectrum Disorder: A Proof of Concept Study (DOI: 10.1089/brain.2016.0483)
This paper has been peer-reviewed and accepted for publication, but has yet to undergo copyediting and proof correction. The final published version may differ from this proof.

Table-III Psychiatric Comorbidity with ASD

Psychiatric Comorbidity (N=15)	**Lifetime**	**Current**
Load of Psychiatric Comorbidity		
Mean #	4 ±2.48	2.40 ±2.69
Range	1-10	0-8
≥2	13 (86.7)	7 (47)
Psychiatric Disorders		
Attention-deficit/hyperactivity disorder (ADHD)	10 (67)	7 (47)
Any Anxiety Disorder	11 (73)	7 (47)
Multiple anxiety disorders (≥2)	6 (40)	4 (27)
Major depressive disorder	11 (73)	6 (40)
Bipolar Disorder (Mania)	6 (40)	1 (07)
Psychosis	3 (20)	3 (20)

Values expressed as N (%) or Mean ±Standard Deviation

Brain Connectivity
Integration and Segregation of Default Mode Network Resting-state Functional Connectivity in Transition-age Males with High-functioning Autism Spectrum Disorder: A Proof of Concept Study (DOI: 10.1089/brain.2016.0483)
This paper has been peer-reviewed and accepted for publication, but has yet to undergo copyediting and proof correction. The final published version may differ from this proof.

Table-IV Whole Brain Seed-voxel Resting-state Functional Connectivity Analysis [Between-group two-sided contrast @ p<0.005 voxel-level and p<0.05 cluster-level FWE-corrected]

DMN Combined Nodes (mPFC, PCC, BL AG, BL ITG)	**BA**	**L/R**	**MNI [x, y, z]**	**Cluster Size**	**t-statistic**
ASD < HC					
AG	39	R*	+60 -62 +33	1678	5.96 [p<0.001]
		L	-51 -67 +41	1488	5.68 [p<0.001}
mPFC	10	R	+04 +57 +26	1311	4.51
ASD > HC					
SMG/pSTG/pAC	40/22/42	R*	+49 -29 +25	1296	-4.43
(l)aVC/FG	19/37	R	+35 -71 +23	2168	-4.39

BA=Brodmann area; MNI=Montreal Neurologic Institute; L=Left; R=Right; (l)=lateral; mPFC=medial Pre-Frontal Cortex; aAG=anterior Angular Gyrus; FG=fusiform gyri; aVC=associative Visual Cortex; pSTG=posterior Superior Temporal Gyrus; SMG=SupraMarginal Gyrus; pAC=primary Auditory Cortex; *Regions constitute the right temporo-parietal junction.

Brain Connectivity
Integration and Segregation of Default Mode Network Resting-state Functional Connectivity in Transition-age Males with High-functioning Autism Spectrum Disorder: A Proof of Concept Study (DOI: 10.1089/brain.2016.0483)
This paper has been peer-reviewed and accepted for publication, but has yet to undergo copyediting and proof correction. The final published version may differ from this proof.

FIGURE CAPTIONS

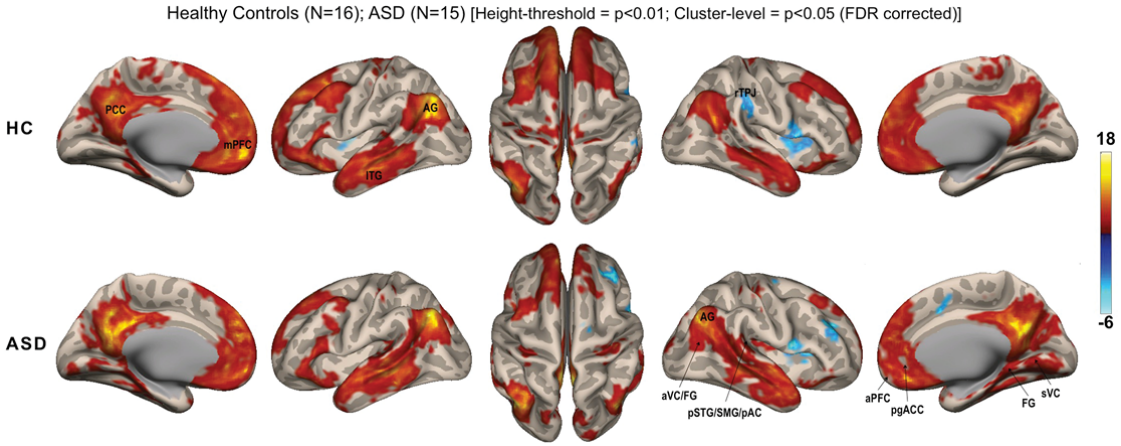

Figure-I.A

Within-group functional connectivity maps of pre-defined DMN seed-voxel whole brain correlation analyses.

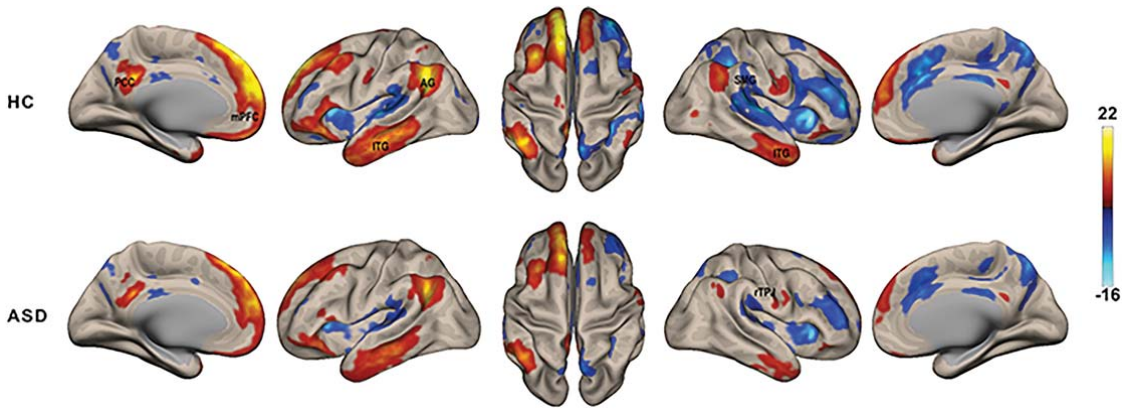

Figure-I.B

Within-group functional connectivity maps of DMN whole brain group ICA (ABIDE data set). TC: N=35; ASD: N=24. Height-threshold whole-brain p<0.001; two-sided FDR corrected; Cluster-level threshold=p<0.05 FWE corrected.

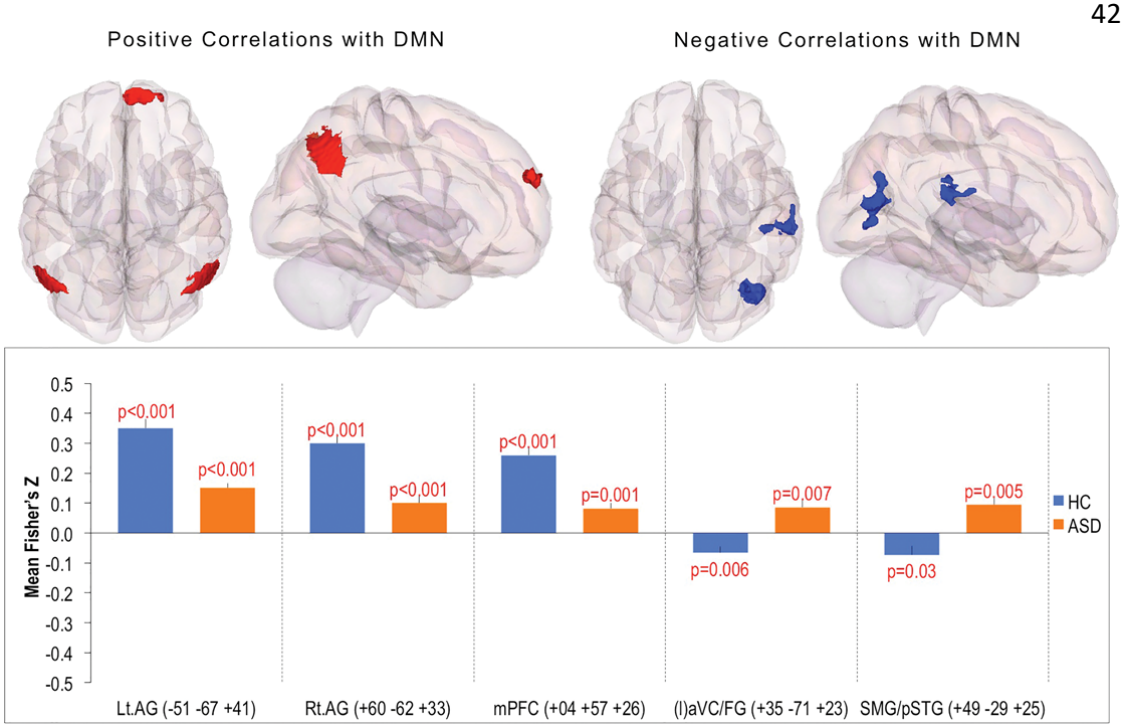

Figure-II.A

Between-group (HC vs. ASD) functional connectivity maps of pre-defined DMN seed-voxel whole brain correlation analyses (whole-brain height threshold of p<0.005).

Brain Connectivity
Integration and Segregation of Default Mode Network Resting-state Functional Connectivity in Transition-age Males with High-functioning Autism Spectrum Disorder: A Proof of Concept Study (doi: 10.1089/brain.2016.0483)
This paper has been peer-reviewed and accepted for publication, but has yet to undergo copyediting and proof correction. The final published version may differ from this proof.

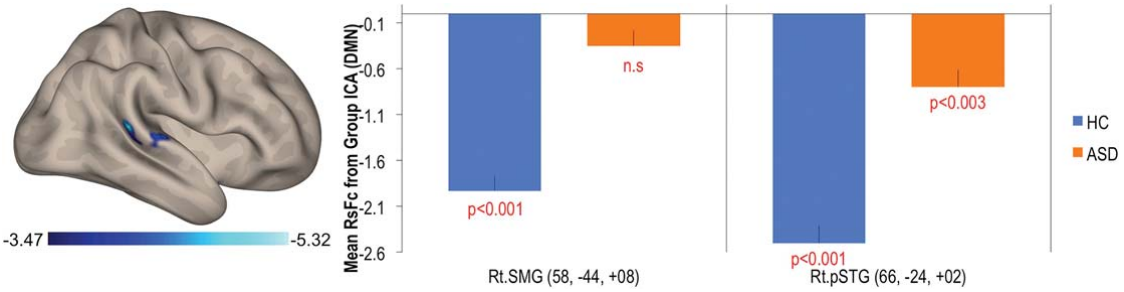

Figure-II.B

Between-group functional connectivity maps of DMN (Group ICA) after regressing out the effect of head motion (ABIDE dataset, height threshold = p<0.001).

Brain Connectivity
Integration and Segregation of Default Mode Network Resting-state Functional Connectivity in Transition-age Males with High-functioning Autism Spectrum Disorder: A Proof of Concept Study (DOI: 10.1089/brain.2016.0483)
This paper has been peer-reviewed and accepted for publication, but has yet to undergo copyediting and proof correction. The final published version may differ from this proof.

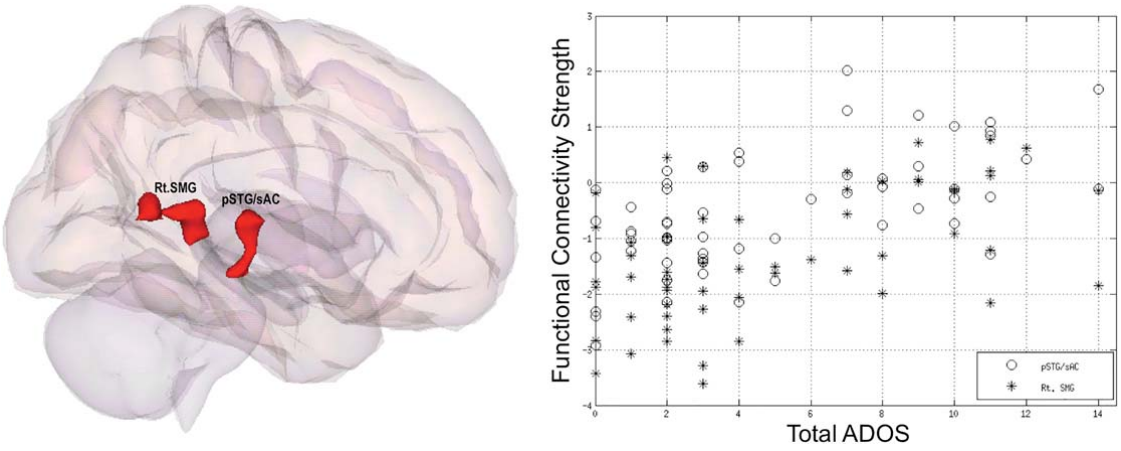

Figure-III

Whole brain ADOS revealed positive correlations (r=0.4) with right SupraMarginal Gyrus (stars) and right posterior Superior Temporal Gyrus (circles) after regressing out the effect of maximum head motion from all the subjects at a height-threshold of whole-brain $p<0.005$ ($p<0.05$ FWE corrected).

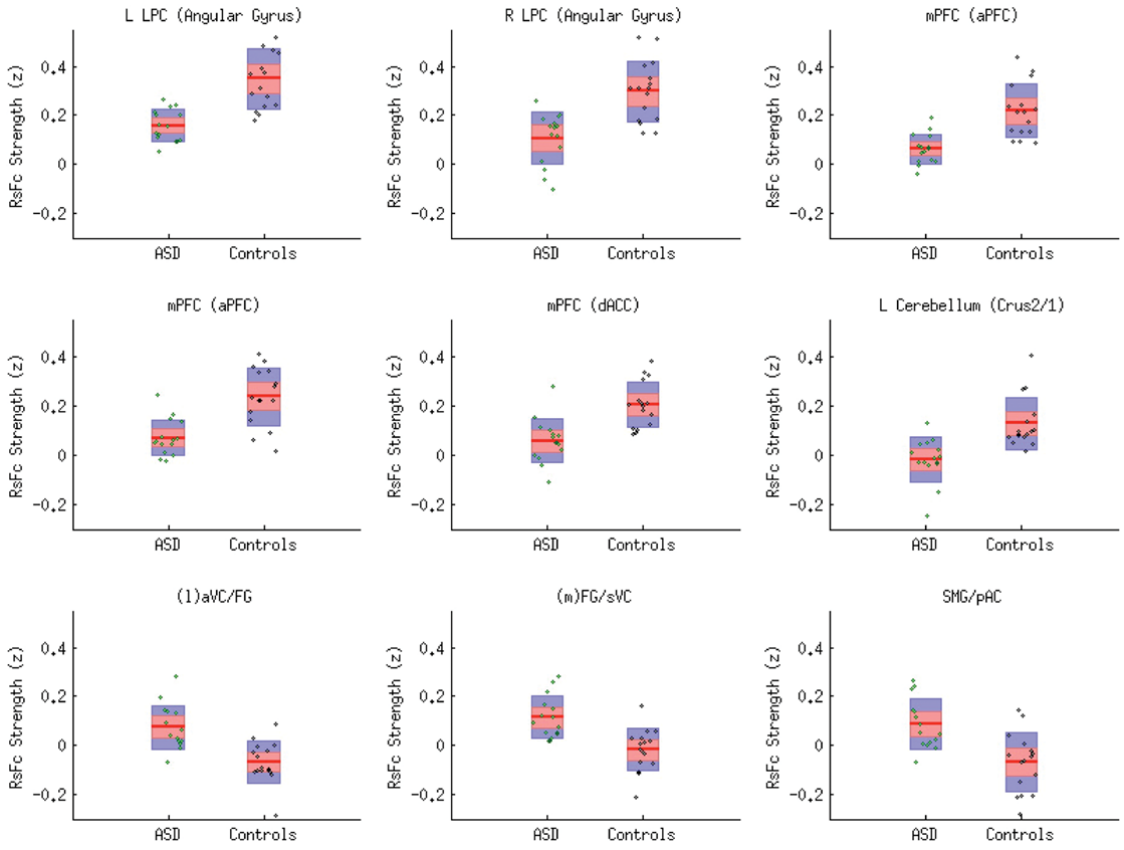

Figure-IV

Box plot representation of the ROIs that survived between-group second-level DMN analysis.

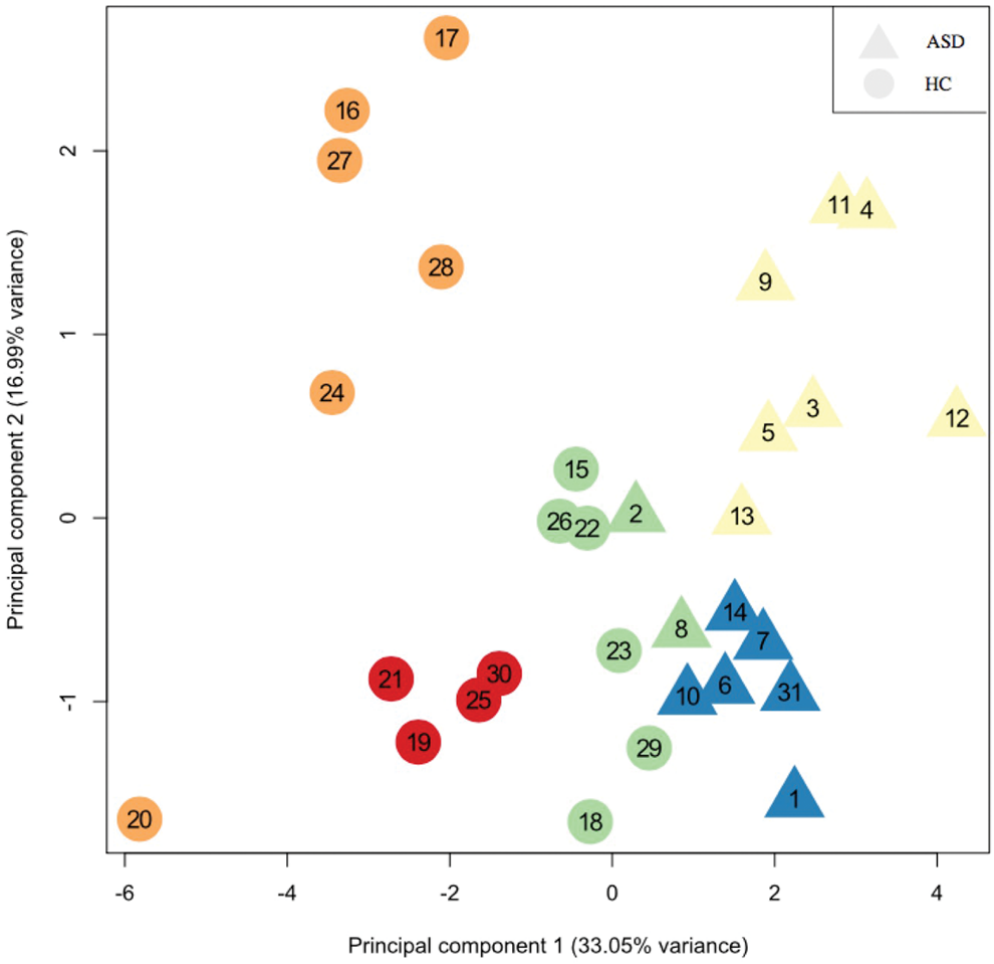

Figure-V.A

Unsupervised clustering of subjects based on the correlation between pre-defined DMN seed and the nine ROIs that survived between-group second-level DMN analysis. First two principal components applied for visualization purpose; each subject identified by numbers; each cluster represented by different color.

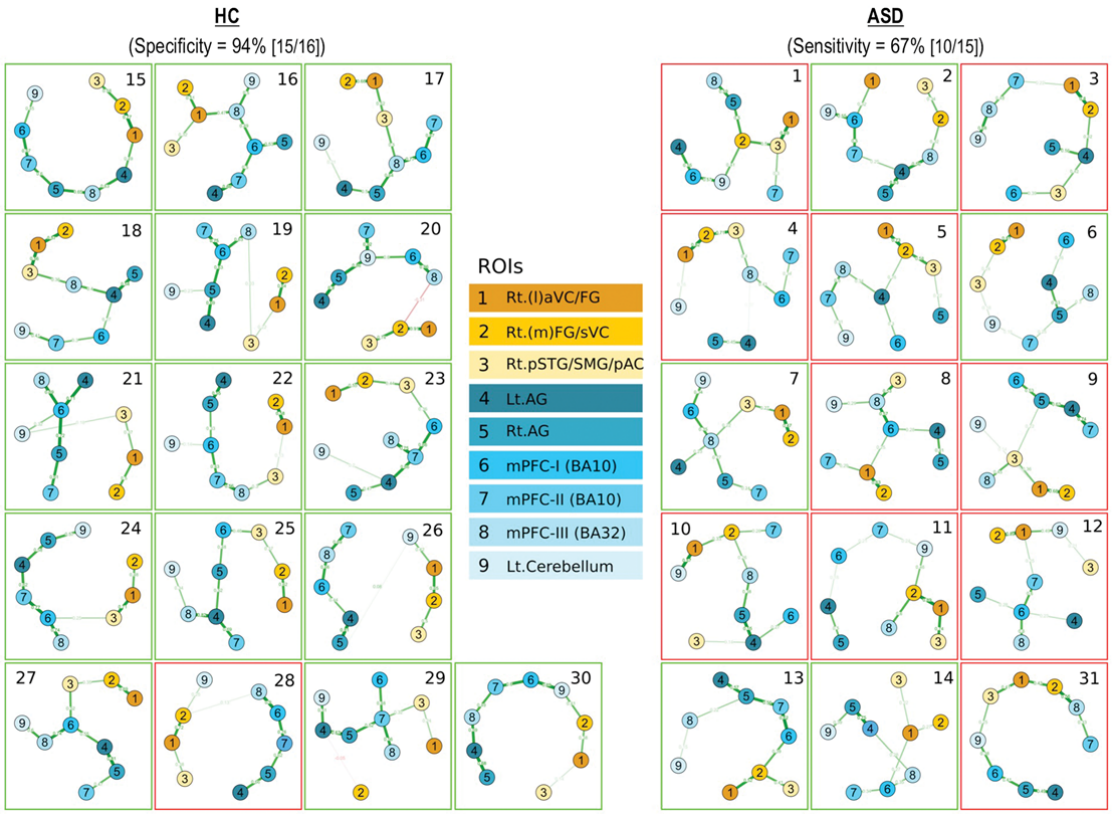

Figure-V.B

Minimum Spanning Tree (MST) of individual subjects from the nine ROIs that survived between-group analysis at the second-level. Shades of blue: Positively correlated nodes with the DMN; Shades of yellow: Negatively correlated nodes with the DMN. Red frame: Atypical topology; Green frame: Typical topology (defined as cohesive cluster of positively correlated nodes).